International Journal of Ambient Energy

ISSN: (Print) (Online) Journal homepage: www.tandfonline.com/journals/taen20

AI control-activated carbon-ZnO/CuO conductive polymer structural super-capacitor for EV

Ataur Rahman & Sany Ihsan

To cite this article: Ataur Rahman & Sany Ihsan (2024) AI control-activated carbon-ZnO/CuO conductive polymer structural super-capacitor for EV, International Journal of Ambient Energy, 45:1, 2427718, DOI: 10.1080/01430750.2024.2427718

To link to this article: https://doi.org/10.1080/01430750.2024.2427718

Published online: 22 Nov 2024.

INTERNATIONAL JOURNAL OF AMBIENT ENERGY
2024, VOL. 45, NO. 1, 2427718
https://doi.org/10.1080/01430750.2024.2427718

Taylor & Francis
Taylor & Francis Group

AI control-activated carbon-ZnO/CuO conductive polymer structural super-capacitor for EV

Ataur Rahman [a] and Sany Ihsan[b]

[a]Mechanical Engineering and Technology, GameAbove Engineering and Technology, Eastern Michigan Engineering, Yapsilanti, MI, USA; [b]Department of Mechanical Engineering, Kulliyyah of Engineering, International Islamic University Malaysia, Kuala Lumpur, Malaysia

ABSTRACT

In the automobile industry, nanocomposite technologies reduce weight and emissions, increasing vehicle energy efficiency. The multipurpose structure of the electric vehicle, known as the structural supercapacitor, is 35% lighter than steel and can produce electricity by trapping solar heat. This work developed an electric double-layer structural supercapacitor (EDLC) using aqueous sodium sulphate (Na2SO4) as the electrolyte, carbon fibre reinforcement conductive polymer (CFRP) and activated carbon zinc oxide (AC ZnO) as the n-type and copper oxide (CuO) as the p-type. Different weight percentages (wt.%) of AC ZnO/CuO capacitors have been constructed and tested at 32°C solar temperatures. Compared to other wt% AC EDLC, the CFRP-EDLC with 6 wt% of AC has the maximum performance, with a capacity of 18.56 μF/cm^2. In comparison to other formulations, the 70 wt% of epoxy, 6 wt.% weight AC and 30 wt% ZnO/CuO EDLC demonstrated superior charging in a shorter amount of time and discharging in a longer amount of time. If the solar trapping heat rises beyond 32°, an AI power management system (AIPMS) has been built into the EDLC EV body panel to prevent any mishaps. Depending on the current EDLC signal, AIPMS indicates EDLC operation.

ARTICLE HISTORY
Received 7 July 2024
Accepted 1 November 2024

KEYWORDS
Nano-composite organic solar capacitor; ACZnO/CuO-doped material; energy efficient; shorter charging time and longer discharging

1. Introduction

Electricity supply of electric vehicles from renewable sources reduces greenhouse gas emissions by 80-95% by 2050 [European Union, EU-28]. However, the extra energy demand of electric vehicles (EVs) causes more carbon dioxide (CO2) emissions and a scarcity of electricity in industry and residence. Renewable energy resources can increaes the total capacity of the electricity mix and decorabonise transportation. Thus, the right candidate like a conductive polymer-based structural panel of EV could be considered as a solar panel to generate and store electricity from solar trapping radiation (heat). It contributes significantly to the EV's mileage extended by sourcing the power of the battery recharge and by reducing the EV's traction power consumption by reducing the EV's weight.

Current research on super-capacitors is focused on increasing power and energy densities and lowering fabrication costs using environment-friendly materials. The core materials studied for super-capacitor electrodes are carbons, metal oxides and conducting polymers. Utra-capacitors are called electrochemical capacitors (ECs) (Chen et al. 2014) have been recently considered as a promising energy storage device and have been applied in various technologies, such as hybrid electric vehicles (HEV) power-supply devices (Rahman et al. 2023; Sun, Cao, and Lu 2012). Nanotechnology is an enabling technology for energy storage. Particularly, carbon nanotubes and graphene sheets have been playing an important role in the development of supercapacitors (Liu et al. 2010; Zhang et al. 2010). Activated carbon materials have a high surface area but unfortunately a low porosity and, therefore, a limited capacitance due to low electrolyte accessibility. A limited energy density (4–5 Wh/kg) and power density (1–2 kW/kg) have been obtained for currently available supercapacitors. Due to its large surface area, high carrier transport mobility and excellent thermal/mechanical stability, graphene has recently been studied as an alternative carbon-based electrode in super-capacitors (Lie, Michael, and Henry 2013; Rahman et al. 2023). Theoretically, the double-layer capacitance value of a graphene electrode can reach up to 550 F/g, the highest value of intrinsic capacitance among all carbon-based electrodes (Carlson et al. 2011; Xia et al. 2009). Recently, supercapacitors with high specific capacitance (276 F/g), power density (20 W/cm^3, 20 times higher than that of the activated carbon counterpart), energy density (1.36 mWh/cm^3, 2 times higher than that of the activated carbon counterpart) (El-Kady et al. 2012; Wu et al. 2010) or metal oxide (Dong et al. 2012) coating to introduce pseudocapacitance. Graphene is an expensive and in this study, it is not considered. Alternatively, ZnO and C nanopowder have been doped for the n-type element of organic capacitor.

1.1. Dielectric material's impact on the capacitance

The mechanical and electrical properties of the dielectric capacitors are affected by the materials of the electrodes and dielectrics and electric breakdown strength (EBD) (Carlson et al. 2011). Electrical breakdown (EBD) occurs when the voltage applied across an electrical insulator exceeds the breakdown voltage and

CONTACT Ataur Rahman mrahma24@emich.edu

current flows through it, which makes the insulator electrically conductive. In the early stages of the research for structural dielectric capacitors, the preliminary test for the energy storage ability of these was demonstrated using carbon fibre reinforcement polymer (CFRP) for conductive electrodes and different papers for dielectric separators. The CFRP electrode layers were manufactured from 0.125 mm thick prepreg weaves. The prepregs were 245 g/m^2 showing a capacitance of 0.193 μF/m^2 and an energy of 0.09 J/g (Carlson et al. 2010).

The main goal of this manuscript is to develop a car panel with an organic CZnO/CuO solar supercapacitor as a potential source of energy generation by trapping the solar heat. However, the potentiality of this technology has been verified by developing a laboratory-scale CZnO (p-type)/CuO (n-type) doped inorganic material into the epoxy resin (ER) and paste over the carbon fibre (CF). The aqueous separator has been sandwiched by the n-type_ER and p-type_ER-doped CF elements.

2. Methodology

The active layer used in polymer solar cells consists of a donor–acceptor blend, where a conjugated polymer acts as a donor. Advanced polymer (ER) has been synthesised for the solar cell by filling the C-ZnO filler powder as a donor (N-type) and the CuO filler polymer acts as an acceptor (p-type). The dielectric material such as paper can be used in between the layers as a partition. In the structure, there are two functional layers, the thin carbon fibre reinforcement C-ZnO filler conductive polymer (n-type) and an Electron Transport Layer (ETL), which conversely has good electron mobility and carbon fibre reinforcement CuO filler conductive polymer (p-type) Hole Transport Layer (HTL), which is characterised by a good hole mobility that tends to act as an electron acceptor.

The negative electrode of the super-capacitor C-ZnO acts as an n-type electrode and has been used to reinforce the carbon fibre. A 70gsm paper dielectric was placed on top and pressed using weight and was left to cure for 24 h. After the n-type electrode carbon fibre hardened, the next layer of carbon fibre patch with wires was placed and the CuO-filled epoxy mixture was pasted on it as a p-type electrode. Finally, CF has been placed on it. A 7% of C doped with 5% ZnO in the negative electrode (n-type) and 5% CuO in the positive (p-type) with CF and dielectric film as a separator as a blocker of the electron mobility through it. Figure 1 shows the schematic diagram of organic supercapacitor.

The CFRP electrodes AC ZnO (n-type) with a band gap energy of 3.2 to 3.4 eV and nano CuO (p-type) with a band gap of 1.2 to 1.8 eV when light falls on the surface. This statement is supported by the authors (Dhara et al. 2016; Carlson et al. 2010). Zinc Oxide (ZnO) nanoparticles were supplied by Chemetal SDN, BHD, Malaysia of size from 10 to 30 nm. The purity level of 99.9% and bulk density of 0.46 ~ 0.55 g/cm^3 Copper (II) Oxide (CuO) nanoparticles were from Sigma-Aldrich the size of 50 nm. The separator materials: 70gsm paper of thickness 0.07 mm for the dielectric capacitor and 20 gsm paper of thickness 0.005 mm (soaked in Na_2SO_4 electrolyte) have been used for the EDLC. The percentage of composition of fillers to make carbon fibre-reinforced conductive polymer organic supercapacitor is shown in Table 1.

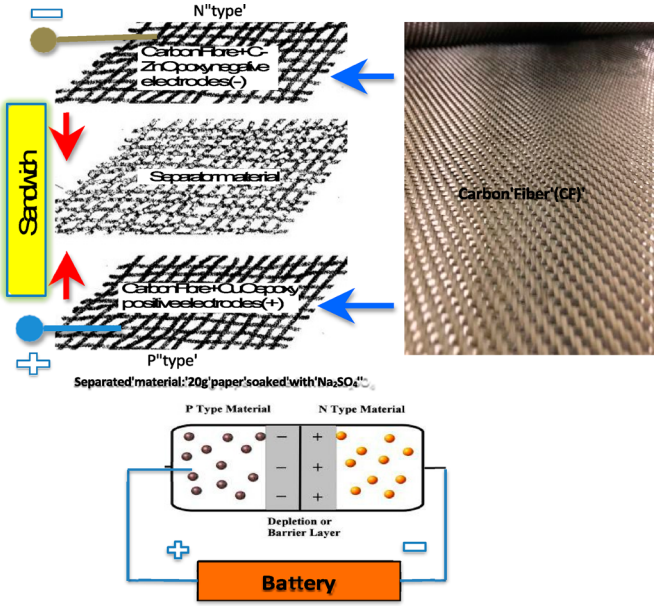

Figure 1. Schematic diagram of the organic super-capacitor.

Table 1. Percentage composition of fillers to make polymer (epoxy) conductive.

	Mixture (wt.%)				
	Mixture 1	Mixture 2	Mixture 3	Mixture 4	Mixture 5
Negative CF electrode					
Epoxy + hardener	95	90	70	64	60
ZnO	5	10	30	30	40
AC	6	10	15	20	25
Positive CFRP electrode					
Epoxy + hardener	95	90	70	64	60
CuO	5	10	30	30	40
AC	6	10	15	20	25

2.1. Mathematical modelling

During the charging period with a solar temperature of 30°C, the energy conversion and storage efficiency as a function of time of charge, t is defined as $\eta_{ecs}(t) = E_{store}(t)/E_{light}(t)$ where E_{store} is the energy stored in the supercapacitor at time t and $E_{light}(t)$ light energy received by the solar cell. The light energy, $E_{store}(t) = P_{light} * t$ where P_{light} is the solar power, the solar power in this study is considered as 1000 W/m^2. The energy store can be defined using the equation (Ataur and Golam 2020)

$$E_{stored}(t) = \int_0^t v_{sc}(\tau) \bullet t_c(\tau)\mathrm{d}\tau \quad (1)$$

where $v_{sc}(\tau)$ is the charging voltage of the capacitor which is developed due to the variation of the solar temperature and the fill factors of the cell and $t_c(\tau)$ is the charging time of the supercapacitor with solar power. Since the supercapacitor is also considered to store the regenerative braking energy, the total energy stored by the supercapacitor can be defined using the equation (Ataur and Golam 2020)

$$E_{T(stored)}(t) = \int_0^t v_{sc}(\tau) \bullet t_c(\tau)\,\mathrm{d}\tau + \int_0^t P_{rgb}(\tau)\mathrm{d}\tau \quad (2)$$

where $P_{rgb}(\tau)$ is the regenerative braking power of the EV which is generated by the motor during deceleration and downing

from the slope. The regenerative braking energy ($E_{rgb}(\tau)$) is considered as 24% of $\frac{1}{2}$ mV^2 where V is the speed of the vehicle in m/s. The current density can be defined (Rahman et al. 2017)

$$J = \left[(N_n \mu_n + N_p \mu_p) E + \left(D_n \frac{\partial N_n}{\partial x} + D_h \frac{\partial N_p}{\partial x} \right)^{(e)} \right] \quad (3)$$

where n represents N-type and p represents P-type, μ the electron mobility of composite, D is the diffusion coefficient, e the electron $= 1.6 \times 10^{-19}$C. The diffusion coefficient is estimated using Einstein's equation, N_n and N_p are the numbers of free electrons. The diffusion coefficient is estimated using Einstein's equation, $D = \mu kT/q$, where k is Bolzmann's constant and q is the charge in Columb. Based on Culomb's law, electric field E induces by an isolate charge q at any point of the photovoltaic panel which can be defined as $E = [q/4\pi\epsilon d^2]$ where D is the thickness of the composition of photovoltaic ZnO and polymer and ϵ is the electrical permittivity of the photovoltaic elements.

The efficiency of the energy conversion of the OPSC can be defined using the following equation (Ataur and Golam 2020),

$$\eta_{ece}(t) = \frac{\int_0^t V_{sc}(\tau) * i_c(\tau) d\tau}{P_{light} * t} * 100\% \quad (4)$$

The time of full charge can be estimated as $t_c = CV_{oc}/I_{sc}$ where V_{oc} is the open circuit voltage and I_{sc} is the short circuit current. The voltage generation of the solar cell can be estimated as $V_{pv} = V_{sc} + R_s I_{sc} = Q_{sc}/C_{sc} + Rs\, I_{sc}$.

3. Result and discussion

Two types of organic capacitors have been made using 6% of C and 5% of ZnO for n-type and 5% of CuO for p-type. A dielectric capacitor with 70 gsm paper of thickness of 0.005 mm as shown in Figure 2(a) and 20 gms paper of thickness of 0.005 mm soaked with Na_2SO_4 for ultracapaciors, as shown in Figure 2(b). The sample's energy storage performances were tested indoors (27°C, fluorescent lamps). Initially, the terminals of the sample have been short -ircuited to ensure no charge is stored in the capacitors. Both capacitors have been tested under bright sunlight of 30°C. A multimetre was attached to the terminals of the samples individually, as shown in Figure 3, voltage readings were taken at an interval of 10 s for 5 min.

The performance investigation of the OSC both in charging and discharging has been conducted at the time for the maximum values of SoC(t), power density and energy density. However, the different discharging times have been recorded for the different wt.% of AC samples, as shown in Table 2.

Figure 4 shows the SoD(t) of the OSC for different wt.% of AC. The wt.% of ZnO for the n-type has been considered constant but only varies the wt.% of AC. The result shows the difference both in charging and discharging for the 5% and 6% of AC. It could be concluded that higher wt.% of AC particles increases the surface area and creates more pores and utilising the polymer (ER) chains to wrap the CFs rather than impregnate AC pores: this resulted in greater specific surface area, especially large micropore area, which enhanced the specific capacitance. Therefore, the OSC can hold the charge for a longer time than the lower percentage of AC. The 40% nano-particle epoxy mixture was too thick to work with mainly because 40wt.% of powders were beyond the saturation point of the epoxy. Overall, the recommended % composition was 30% ZnO in the negative electrode and 30%CuO in the positive electrode.

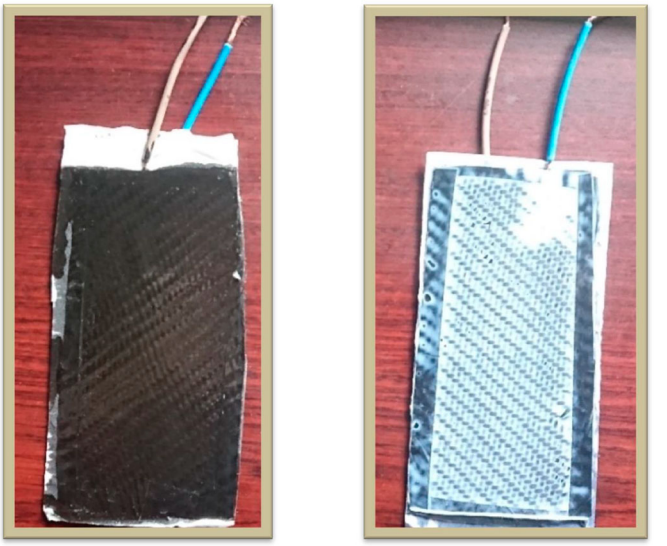

Figure 2. Organic capacitor (a) dielectric capacitor with 70 gsm paper of thickness of 0.005 mm (b) Ultra-capacitor with 20 gsm paper of thickness of 0.005 mm (soaked in Na_2SO_4).

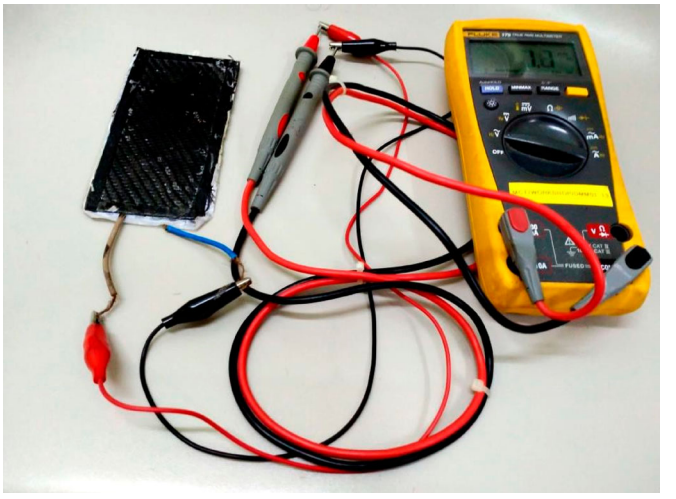

Figure 3. AC-ZnO/CuO solar-dependent capacitor testing at 32°C solar heat.

Table 2. Performance of the ZnO/CuO organic capacitor at different levels of AC.

CF electrodes	Mixture 1 (wt.%)	Mixture 2 (wt.%)	Mixture 3 (wt.%)	Mixture 4 (wt.%)	Mixture 5 (wt.%)
Epoxy & hardener	95	90	70	64	60
ZnO/CuO	5	10	30	30	40
AC	2	3	4	6	7
Verdict	Poor performance	In the middle	Best performance	Mixed performance	Did not work

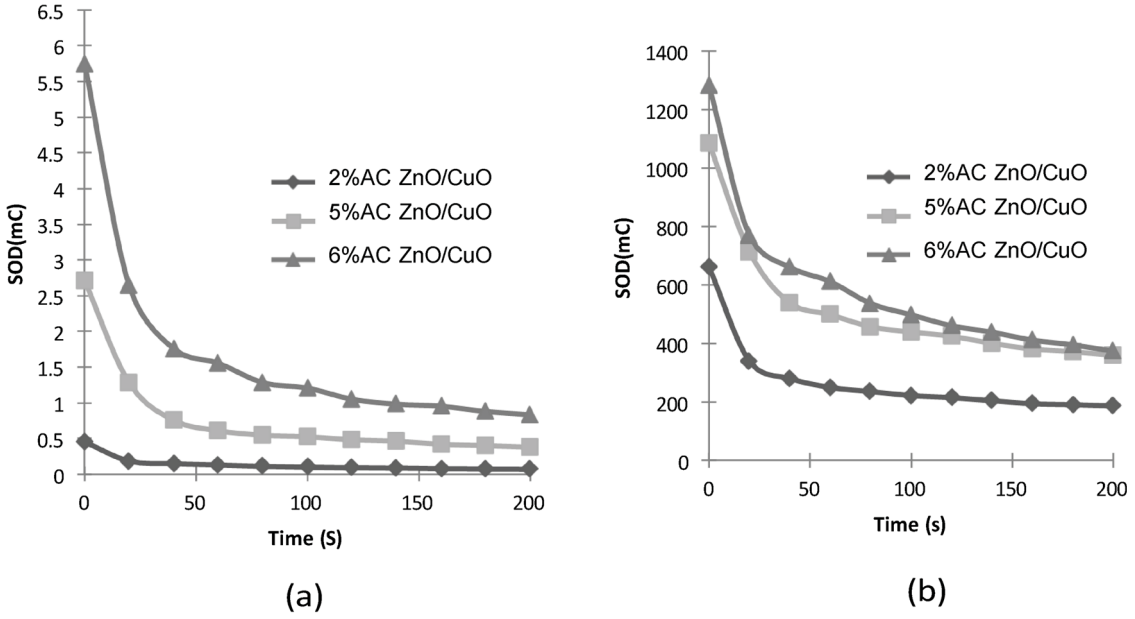

Figure 4. SOD (t) (a) Dielectric Capacitor (left), (b) EDLC (right).

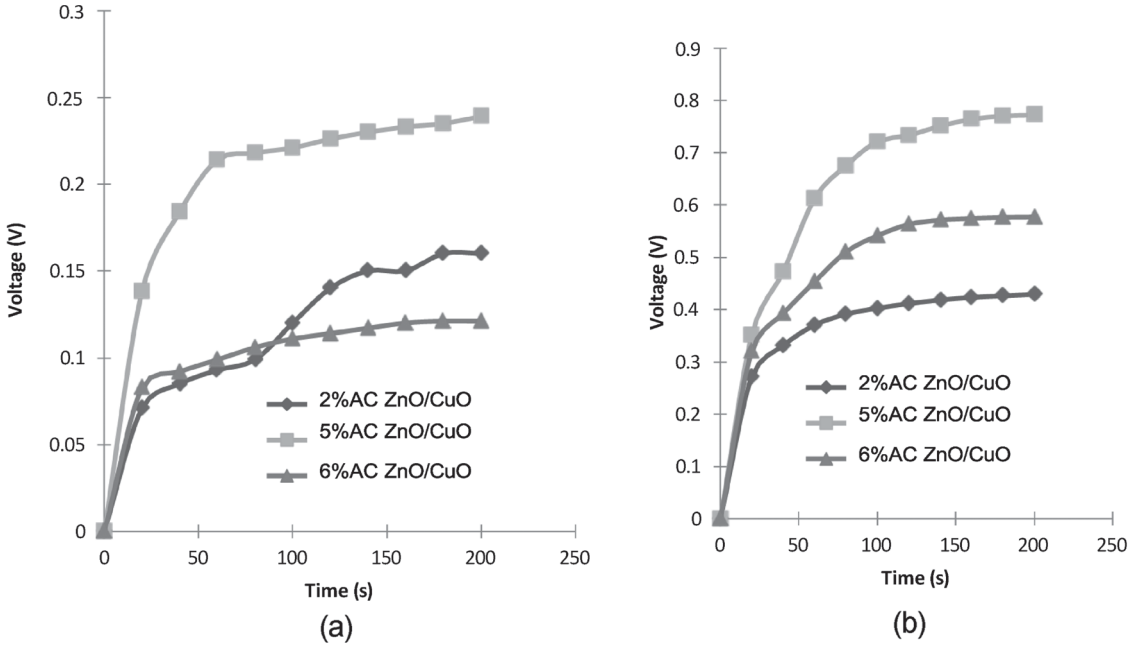

Figure 5. Charging voltage of the OSC.

3.1. Energy storage parameters

All samples have been charged with solar heat at 32°c fraction of a second. Solar charging voltage was taken for 1 min in every 10 s. Discharging reading has been taken for 5 min in every 10 s. The capacitance measured is as follows.

Figures 5–6 show that the 6% Al-30% ZnO/CuO has the highest voltage in charging and voltage drop with respect to time is the lowest among all compositions. This is due to the more porosity and ionisation capacity of EDLC. It could be concluded that wt.% of AC particles increases the surface area and creates more pores and utilising the polymer (ER) chains to wrap the CFs rather than impregnate AC pores: this resulted in greater specific surface area, especially large micro-pore area, which enhanced the specific capacitance. Therefore, the wt.% AC OSC can hold the charge for a longer time than the lower percentage of AC. Furthermore, the 40% nano-particle epoxy mixture was too thick to work with mainly because of beyond the saturation point (resistance) of the epoxy. Overall, the recommended 30 wt.% ZnO in the negative electrode and 30%CuO in the positive electrode is the best for the organic capacitor.

Table 3 shows that EDLC can store much higher capacitance than dielectric OSC. However, 6 wt%% AC 30 wt% % ZnO/CuO 20 gsm paper soaked in Na_2SO_4 EDLC has a capacitance of 522 micro-Farad (μF) while 30 wt% % ZnO/CuO 70 gsm paper capacitance of 0.098 (μF). The EDLC has shown higher capacitance due to the higher movement of an electron through the external

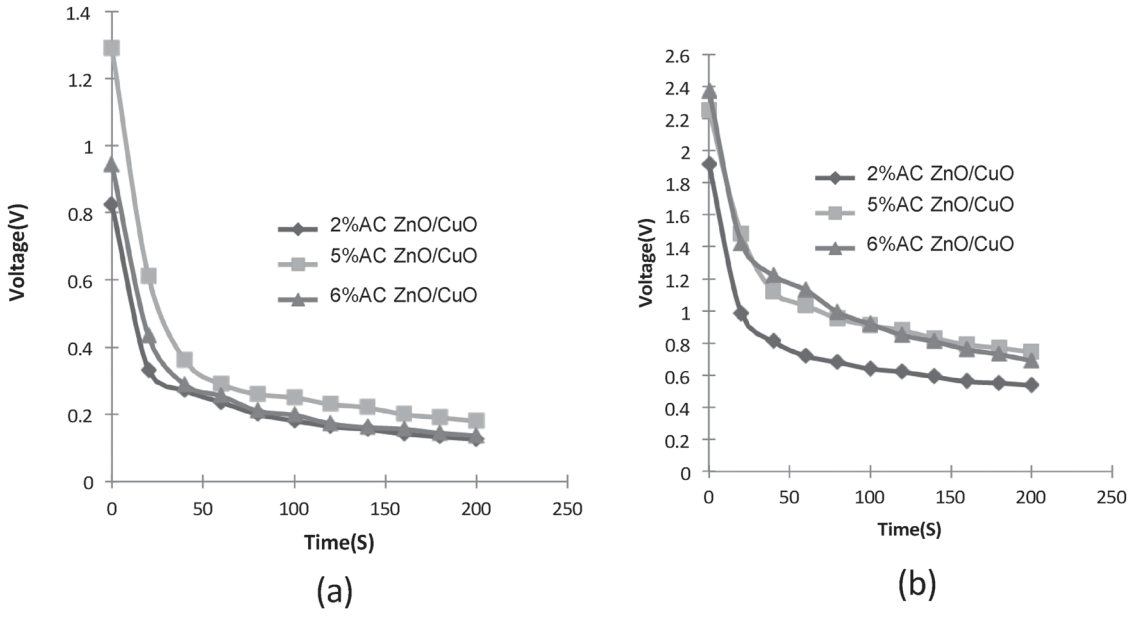

Figure 6. Discharging voltage of OSC (c) Dielectric capacitor, (b) Ultracapacitor.

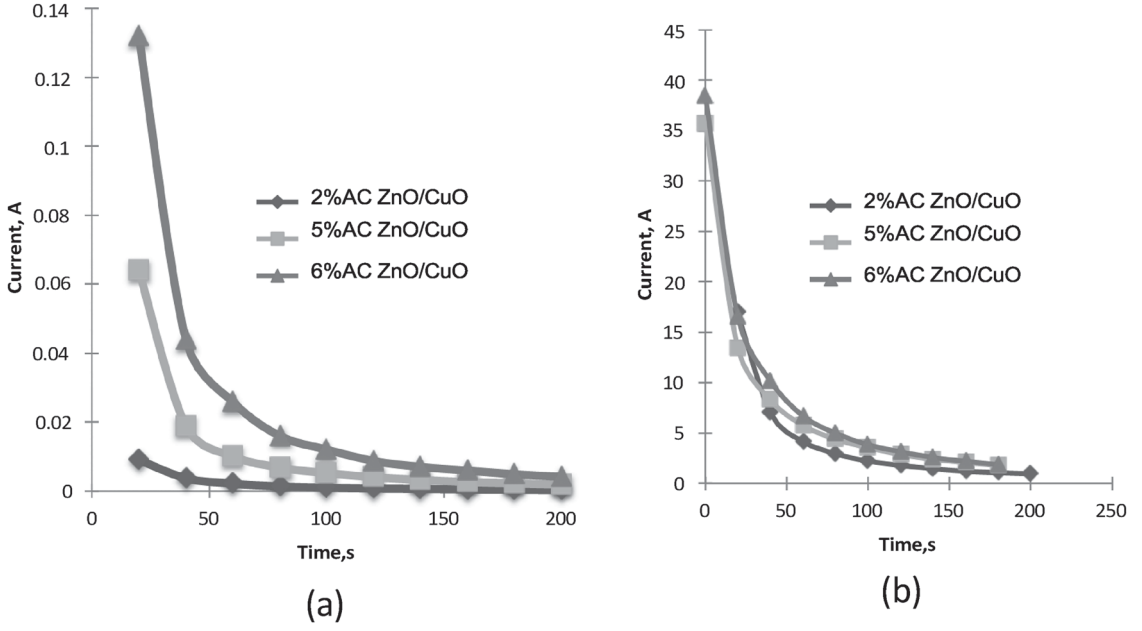

Figure 7. Current flow (a) Dielectric (b) EDLC.

Table 3. The capacitance of solar-dependent capacitor at 32^0C solar heat (Ataur and Golam 2020).

Capacitance of Al ZnO/CuO solar capacitor				
(i) Dielectric capacitor with 70 gsm paper				
	2% AC ZnO/CuO	3% AC ZnO/CuO	5% AC ZnO/CuO	6% AC ZnO/CuO
Capacitance(μF)	0.41	0.45	9.3	0.098
(ii) Ultra-capacitor 20 gsm paper soaked in Na_2SO_4 electrolyte				
	2% AC ZnO/CuO	3% AC ZnO/CuO	30% AC ZnO/CuO	30% AC ZnO/CuO
Capacitance(μF)	357	476	503	522

circuit, greater specific surface area and aquous Na_2SO_4 accelerating the fast electrolysis compared with non-aqueous and non-utilised AC.

Figures 7–8 show that 6%AC-30%ZnO/CuO EDLC has higher performance in terms of current and current density compared to the current density of dielectric capacitor. This happened due to the higher charge transfer of ACZnO/CuO through the lower resistance of aqueous Na_2SO_4 20 gsm paper.

Table 4 shows the overall performance of AC-ZnO/CuO conductive polymer carbon fibre-reinforced OSC. Power density and energy density are important causes compared to the size and weight of the energy storage device. The performance of 20% AC was poor because of the light film creation with the ZnO this might affect the overall performance due to the lowest interstitial space. The result shows the energy density of the OSC decreases with increasing the wt.% of AC, which closes the interstitial space of the filler of ZnO with the PVDF. The result implies that due to the densely mixed AC, the

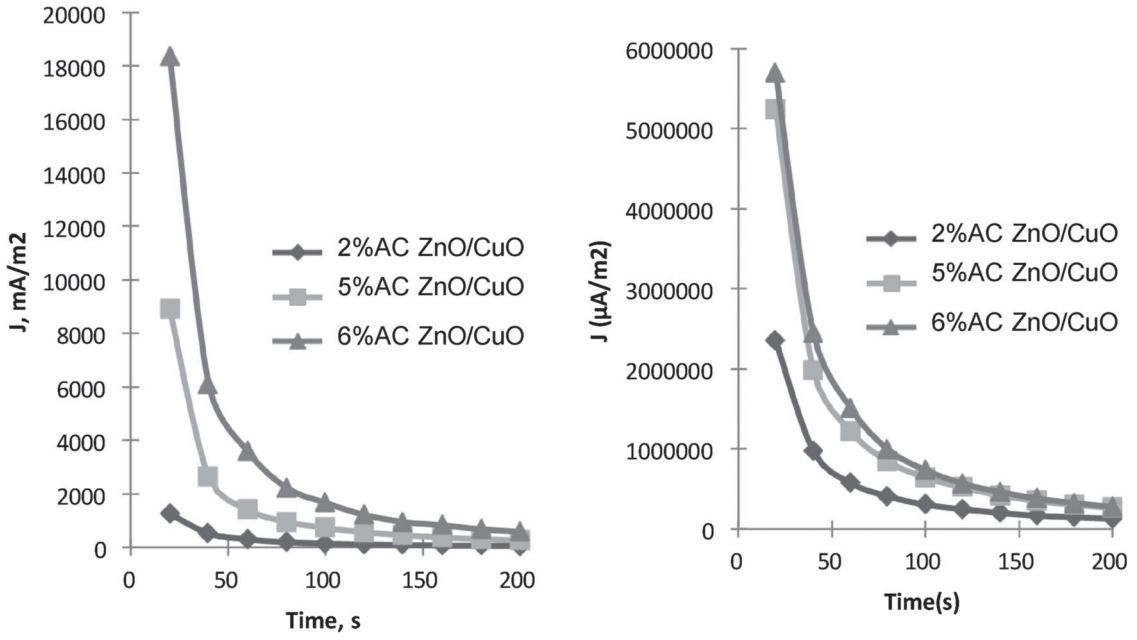

Figure 8. Current density (a) Dielectric, (b) EDLC.

Table 4. Overall performance of the AC electrode in different wt%.

C (%)	Voltage (V_{oc})	Capacitance C(μF/cm^2)	Current density J_{sc}(A/cm^2)	Power density P_{ms}(kWkg^{-1})	Energy Density E_{ms}(W.hkg^{-1})
6	2.414	13.356	2.234	18.691	5.198
10	2.349	12.356	2.013	17.747	4.707
15	2.338	12.156	2.084	17.859	3.85
20	2.154	11.27	1.312	5.863	1.623

Table 5. Different electrodes for EDLC and their properties.

Carbonaceous material	Electrolyte	Double-layer capacitance (μF/cm^2)	Surface Area g/m^2	Reference
Published product				
Activated carbon	10% NaCl	19	1200	Iro, Subramani, and Dash (2016)
Carbon black	1 M H_2SO_4 3.1 wt.% KOH	8 ∼ 10	230	
Graphite powder	10% NaCl	35	4	
Graphite cloth	0.168N NaCl	10.7	630	
Carbon aerogel	4M KOH	23	650	
Researcher products: (ACZnO/CuO with 20 gsm paper soaked in Na_2SO_4)				
AC 6%	1M Na_2SO_4	18.56	1050	Authors Experimental Result
AC10%		13.35		
AC15%		13.156		
AC20%		11.27		

Table 6. Different electrodes for EDLC and their properties.

Electrode	Electrolyte	Power density (kW/kg)	Energy density (Wh/kg)	Reference
Published product [Porous carbon (PC), Surface area (SA)]				
PC, SA1496 m^2/g	6M KOH	4.2	3.3	Razaq et al. (2012)
Graphene aerogel	6M KOH	7	45	Pushparaj et al. (2007)
B-doped rGO	0.5 M H_2SO_4	10	5.5	Yu et al. (2011)
Graphene nanoribbon	1 M H_2SO_4	9.7	4.10	Chen et al. (2011)
Researcher products [AC, Surface area (SA)]				
AC6%, SA1050 m^2/g	1M Na_2SO_4	18.691	5.198	Authors' Experimental Result
AC10%, SA1050 m^2/g		16.74	7.707	
AC 15%, SA1050 m^2/g		15.85	8.85	
Activated Carbon 20%, 1050 m^2/g		5.863	1.623	

Table 7. Comparison with other research.

Composite	V_{oc} (V)	I_{sc} (A/m^2)	Efficiency (%)	Reference
AC-ZnO/CuO (6%AC ZnO / CuO)	0.779	220.59	5.71	Authors' results
CuO/ZnO	0.63	180	4.48	Dhara et al. (2016)
SnS/ZnO	0.12	0.4	0.003	Dhara et al. (2016)
CdS/SnS	0.26	96	1.3	Dhara et al. (2016)

micro-pore area became a film, thus it closed the energy gap in electrons.

The performance of the developed OSC has been compared with the published research work (Gupta and Miura 2006; Shaheer and Rahman 2021) as shown in Table 5. The AC for the surface area 1200 g/m^2 has shown a capacitance of 19 miF/cm^2 (Iro, Subramani, and Dash 2016) which is slightly less than the authors' experimental result for 1050 g/m^2 shows the capacitance of 18.56 miF/cm^2. It could be mainly for the surface area of 14% less of authors compared (Khan et al. 2023; Niu et al. 2012).

Table 6 shows the difference between the EDLC (authors) with the published works. The authors' EDLC has shown better

performance than the authors' (Lu, Li, and Tong 2015; Razaq et al. 2012; Zhang and Zhao 2009) except the author product SWNT.

Table 7 shows the performance comparison of the authors' EDLC of wt.% 6 AC wt.%30 ZnO/CuO in terms of V_{OC}, I_{SC}, and efficiency is found better than the authors' (Dhara et al. 2016). However, an extensive experimental study is required to test the EDLC with the EV as a body panel for its validation.

4. Power management system (PMS): ANFIS

4.1. Algorithm of ANFIS Control solar OSSC

Artificial Intelligence (AI) is a branch of computer science able to analyse large-scale data. ANNs, ANFIS techniques and FLC are types of AI techniques. The two methods of ANN training, are supervised training and unsupervised training. Supervised training needs a set of inputs and the desired output of the network, while unsupervised training requires only the input of the network and ANN is supposed to classify the data properly (Rahman, Afroz, and Jafar 2019).

ANFIS is a kind of ANN that is based on the Takagi–Sugeno fuzzy inference system. Since it combines both neural networks and fuzzy logic principles, it can capture the benefits of both in a single framework. Its inference system corresponds to a set of fuzzy IF-THEN rules that have the learning capability to estimate nonlinear functions. Hence, ANFIS is considered to be a universal estimator. ANFIS control is a hybrid method consisting of two parts which are the gradient method applied to calculate input membership function parameters and the least square method applied to calculate the parameters of the output function. The structure of ANFIS is shown in Figure 9.

ANFIS is a simple machine learning technique, where Fuzzy Logic is utilised to transform random inputs into a specified output via extremely interconnected Neural Network processing information and element connections. Then these are weighed to map the numerical inputs into an output. In ANFIS, Neural Network learning methods are utilised to regulate the parameters of a Fuzzy Inference System (FIS). A first-order Sugeno model with two fuzzy 'If-Then' rules can express the ANFIS configuration with the following rules and equations:

$$\text{Rule}(1): \text{IF} x \text{is} a_1 \text{AND} y \text{is} b_1, \text{THEN} \quad f_1 = p_1 x + q_1 y + r_1 \tag{5}$$

$$\text{Rule}(2): \text{IF} x \text{is} A_2 \text{AND} y \text{is} B_2, \text{THEN} \quad f_2 = p_2 x + q_2 y + r_2 \tag{6}$$

where x_i and y_i are the inputs, a_i and b_i are the fuzzy sets, f_i are the outputs specified by the fuzzy rule and p_i, q_i, and r_i are the design parameters that are determined during the training process.

The configuration of ANFIS is fixed with many parameters, which causes a tendency for the system to overfit the data on which it is trained, especially with a large number of training epochs. The trained FIS may not adapt effectively to other independent data sets if overfitting occurs. For an ideal situation, the efficiency of the converters is 0.9. For solar power, it is represented as an equation.

$$\text{Ideal} P_{\text{solar}} = [V_{\max} * V_{\text{Series}}] * [I_{\max} * N_{\text{parallel}}] \tag{7}$$

where P_{solar} is the power generated by solar panels, $V_{\max}$ is the maximum voltage, N_{sries} is the number of solar modules in series, $I_{\max}$ is the maximum current and N_{parallel} is the number of solar modules in parallel.

The ideal power of the battery is determined by the following equation and the ideal power of the supercapacitor is determined by the equation:

$$I_{\text{deal}} P_{\text{battery}} = V_{\text{battery}} * I_{\text{battery}} \tag{8}$$

$$\text{Ideal} P_{\text{sc}} = V_{\text{sc}} * I_{\text{sc}} \tag{9}$$

Power simulation has been conducted for the body panel of EV made with EDLC (6wt.% AC 30 wt.% ZnO/CuO) using the Simulink model, as shown in Figure 10. It is assumed that the power of the EV such as starting system, lighting system, instrumentation system, wiper motor, power windows motor and air-conditioning power will be met by the power of the EDLC body

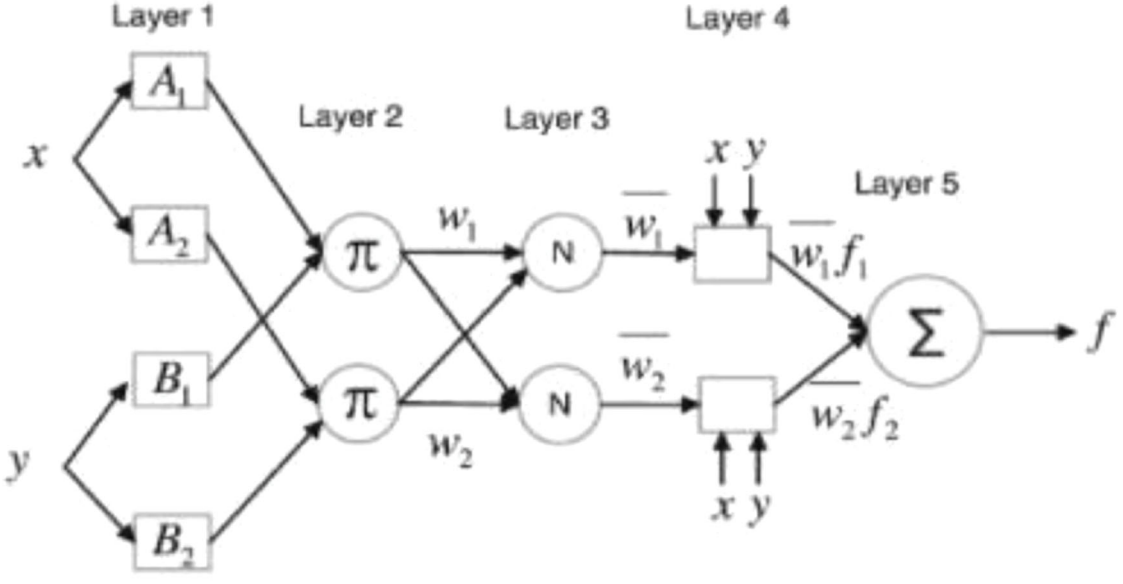

Figure 9. Architecture of the ANFIS system.

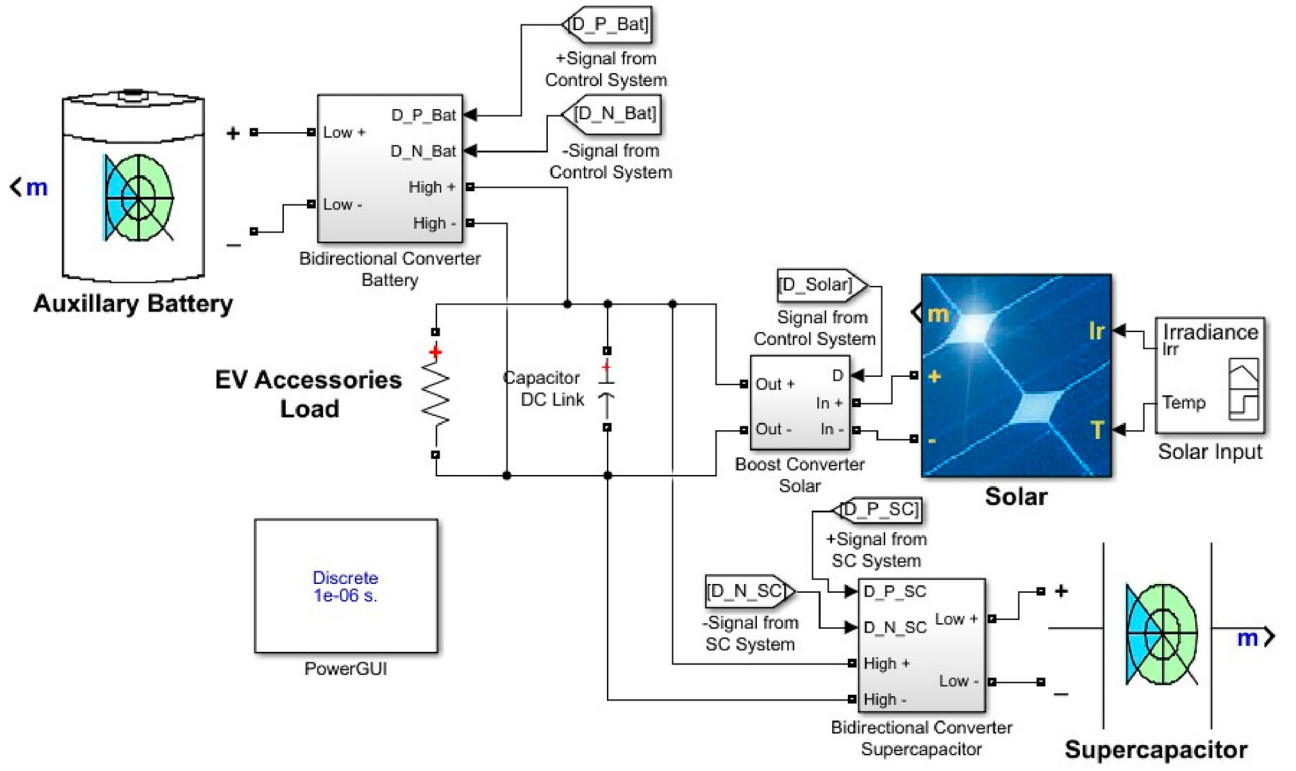

Figure 10. Simulation model (Ataur and Golam 2020).

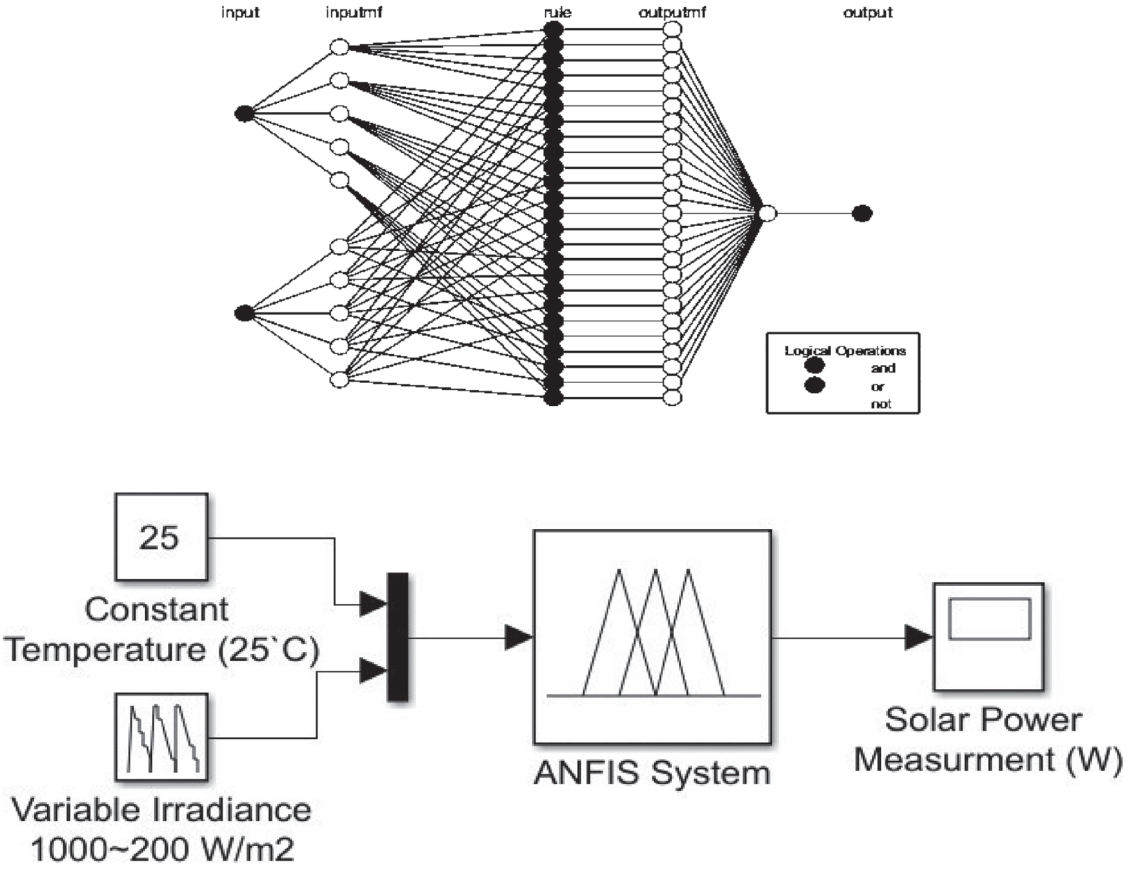

Figure 11. ANFIS simulation for P_{solar} (Ataur and Golam 2020).

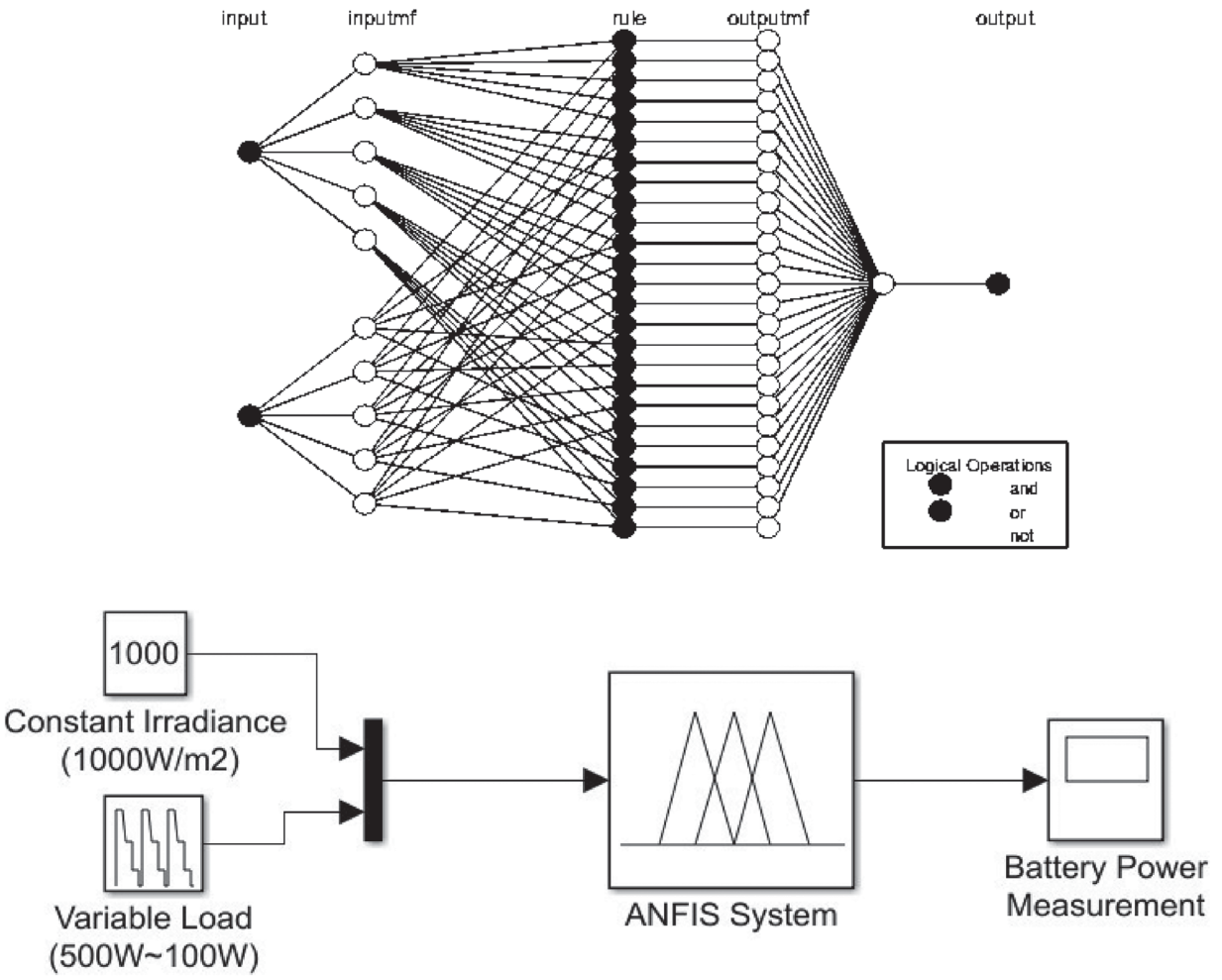

Figure 12. Simulation of the $P_{battery}$ ANFIS System (Ataur and Golam 2020).

Table 8. Solar power simulation results from simulink (OSSC size of 9.75 m^2) (Ataur and Golam 2020).

Input parameter		Output parameter
Temperature(°C)	Irradiance(W/m^2)	P_{solar} (W)
25	1000	957.1
25	800	729.1
25	600	584.1
25	400	388.4
25	200	180.8

Table 9. Battery power simulation results from simulink (Ataur and Golam 2020).

Input parameters		Output
Irradiance (W/m^2)	Load (W)	$P_{battery}$ Discharge (W)
1000	500	−375.6
1000	400	−453.4
1000	300	−525.4
1000	200	−610.8
1000	100	−705.3

panel. Solar power is simulated by the product of solar panel voltage (V_{OC}) and current density (I_{SC}). To test the efficiency of the solar supercapacitor in the real-life cycle, input irradiance is set as variable irradiance in the range of 200–2000 W/m^2 at 25°C to get the output power from the solar supercapacitor in the range of 180–1000 W, as presented in Table 8. The main objective of the power management system of the EDLC is to protect the n-type (AC ZnO) and p-type (CuO) semi-conductive elements from overheating due to the higher electro-chemical reaction and heat development. Thus, if the PMS_ANFIS make the EDLC connect to the ground, the excessive power will go to the ground and make EDLC friendly to generate and store energy as an auxiliary battery required, as shown in Figure 11.

The simulated result that has been obtained from the Simulink model based on the organic structural solar super-capacitor panel and, the constant temperature of 25°C, solar input irradiance in the range of 200–1000 W/m^2 has presented Table 9 while using the output parameter the ANFIS structure, as shown in Figure 12. There are two inputs, irradiance and load and one output, $P_{battery}$. Irradiance input has 5 membership functions (constant 1000 W/m^2) and Load input has 5 membership functions based on the load of the EV's electrical system (500 ~ 100 W).

For real-life applications of solar supercapacitors, input irradiance will vary for the geographical location of the application. The solar irradiance profile is set as 1000 W/m^2 for 30% of total time, 600 W/m^2 for 30% of total daytime, 200 W/m^2 for 30% of the total day time and 0 W/m^2 (No Sunlight) for 10% of the total day time. Signal statistics from Simulink show that the mean solar power over one specific period is 495.4 W, as shown in Figure 13.

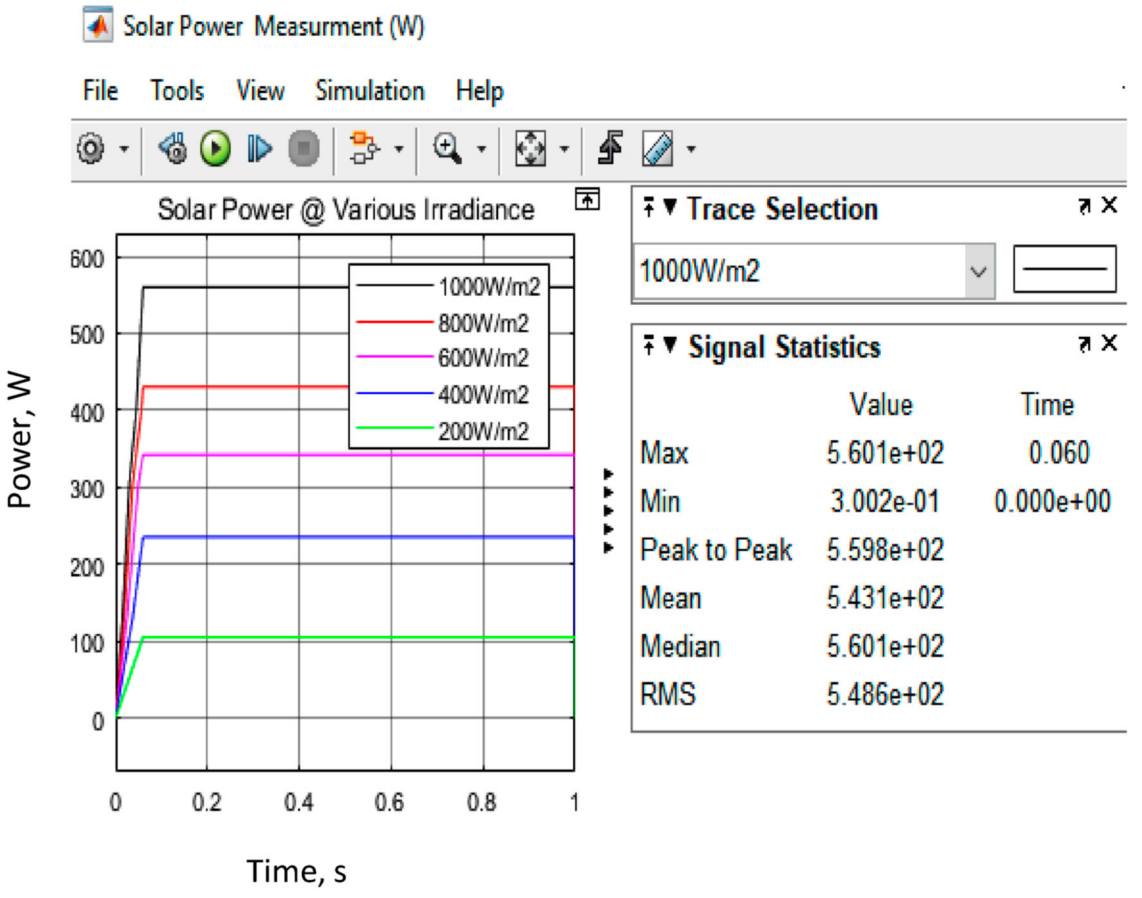

Figure 13. Solar power at different irradiance settings by ANFIS.

5. Conclusion

The development of EV body panels using organic n-type (AC ZnO) and p-type (CuO) semi-conductive elements has been studied. The conclusions have been provided based on the research output of this study:

- Organic EDLC discharging takes a longer time than charging which is due to ER doped with AC ZnO /CuO holding the charge for a longer time into its larger micro-pore area.
- The maximum strength of the organic EDLC has been verified compared with some of the published works and found it has enough to sustain with any external load. Thus, this study shows that it has a unique novelty in generating and storing the energy from trapping the solar heat without interrupting its performance in any instant of solar heat-trapping.
- A power management system (PMS) has been incorporated with an EDLC body panel to avoid if any incident happens due to the high trapping of solar heat. AI _PMS will signify the operation of the EDLC based on the current signal of the EDLC.

Acknowledgements

The authors express their gratitude to Eastern Michigan University in Ypsilanti, Michigan, USA, for enabling them to continue their research and to the Research Management System at International Islamic University for funding this project. The laboratory technician's assistance in the development of this project is also appreciated by the authors.

Disclosure statement

No potential conflict of interest was reported by the author(s).

ORCID

Ataur Rahman http://orcid.org/0000-0001-5494-0610

References

Ataur, R., and K. Golam. 2020. "Al-ZnO / CuO_CFRP Organic Structural Auxiliary Energy Storage System for Electric Vehicle." *Solid State Science and Technology* 28 (1 & 2): 103–116.

Carlson, T., D. Ordéus, M. Wysocki, and L. E. Asp. 2010. "Structural Capacitor Materials Made from Carbon Fibre Epoxy Composites." *Composites Science and Technology* 70 (7): 1135–1140. https://doi.org/10.1016/j.compscitech.2010.02.028.

Carlson, T., D. Ordéus, M. Wysocki, and L. E. Asp. 2011. "CFRP Structural Capacitor Materials for Automotive Applications." *Plastics, Rubber and Composites* 40 (6-7): 311–316. https://doi.org/10.1179/174328911X12948334590286.

Chen, C. C., W. H. Chang, K. Yoshimura, K. Ohya, J. You, Z. Hong, and Y. Yang. 2014. "An Efficient Triple-junction Polymer Solar Cell Having a Power Conversion Efficiency Exceeding 11%." *Advanced Materials* 26 (32): 5670–5677. https://doi.org/10.1002/adma.201402072.

Chen, W., R. B. Rakhi, L. B. Hu, X. Xie, Y. Cui, and H. N. Alshareef. 2011. "High-performance Nanostructured Supercapacitors on a Sponge." *Nano Letters* 11 (12): 5165–5172. https://doi.org/10.1021/nl2023433.

Dhara, A., S. Bibhutibhushan, B. Apurba, C. Sumit, and M. Nillohit. 2016. "Core-Shell CuO-ZnO p-n Heterojunction with High Specific Surface Area for Enhanced Photoelectrochemical Energy Conversion." *Solar Energy* 135:327–332.

Dong, X., X. Wang, J. Wang, H. Song, X. Li, L. Wang, and P. Chen. 2012. "Synthesis of a MnO_2–Graphene Foam Hybrid with Controlled MnO_2 Particle Shape and its Use as a Supercapacitor Electrode." *Carbon* 50 (13): 4865–4870. https://doi.org/10.1016/j.carbon.2012.06.014.

El-Kady, M. F., V. Strong, S. Dubin, and R. B. Kaner. 2012. "Laser Scribing of High-performance and Flexible Graphene-based Electrochemical Capacitors." *Science* 335 (6074): 1326–1330. https://doi.org/10.1126/science.1216744.

Gupta, V., and N. Miura. 2006. "Polyaniline/Single-wall Carbon Nanotube (PANI/SWCNT) Composites for High Performance Supercapacitors." *Electrochimica Acta* 52 (4): 1721–1726. https://doi.org/10.1016/j.electacta.2006.01.074.

Iro, Z. S., C. Subramani, and S. S. Dash. 2016. "A Brief Review on Electrode Materials for Supercapacitor." *International Journal of Electrochemical Science* 11 (12): 10628–10643. https://doi.org/10.20964/2016.12.50.

Khan, Shaheer Ahmed, Ataur Rahman, Wajahat Khan, and Syed Mustafa Haider. 2023. "Characterization and Application of Nano-composite Zinc Oxide /Poly Vinyl Alcohol Thin-film in Solar Cell Performance Enhancement." *Journal of Mechanical Science and Technology* 37 (10): 137–144.

Lie, M., B. J. Michael, and J. Henry. 2013. "Efficient Planar Heterojunction Perovskite Solar Cells by Vapour Deposition." *Nature* 501746:395–398.

Liu, C., Z. Yu, D. Neff, A. Zhamu, and B. Z. Jang. 2010. "Graphene-based Supercapacitor with an Ultrahigh Energy Density." *Nano Letters* 10 (12): 4863–4868. https://doi.org/10.1021/nl102661q.

Lu, X. F., G. R. Li, and Y. X. Tong. 2015. "A Review of Negative Electrode Materials for Electrochemical Supercapacitors." *Science China Technological Sciences* 58 (11): 1799–1808. https://doi.org/10.1007/s11431-015-5931-z.

Niu, Z. Q., P. S. Luan, Q. Shao, H. B. Dong, J. Z. Li, J. Chen, D. Zhao, et al. 2012. "A "Skeleton/Skin" Strategy for Preparing Ultrathin Free-standing Single-walled Carbon Nanotube/Polyaniline Films for High Performance Supercapacitor Electrodes." *Energy & Environmental Science* 5 (9): 8726–8733. https://doi.org/10.1039/c2ee22042c.

Pushparaj, V. L., M. M. Shaijumon, A. Kumar, S. Murugesan, L. Ci, R. Vajtai, R. J. Linhardt, O. Nalamasu, and P. M. Ajayan. 2007. "Flexible Energy Storage Devices Based on Nanocomposite Paper." *Proceedings of the National Academy of Sciences* 104 (34): 13574–13577. https://doi.org/10.1073/pnas.0706508104.

Rahman, Ataur, Rafia Afroz, and Abdul Hassan Jafar. 2019. *Green Transportation System*. 1st ed. Kuala Lumpur: IIUM Press, International Islamic University Malaysia. ISBN 978-967-491-021-1.

Rahman, Ataur, Kyaw Myu Aung, Khalid Saifullah, and Mizanur Rahman. 2017. "Physics of ZnO/SiO_2 Electrolyte Semi-conductive Thermal Electric Generator." *International Journal of Advanced and Applied Sciences* 4 (5): 35–40. https://doi.org/10.21833/ijaas.2017.05.006. ISSN 2313-626X E-ISSN 2313-3724.

Rahman, A., K. Myo Aung, S. Ihsan, R. M. Raja Ahsan Shah, M. Al Qubeissi, and M. T. Aljarrah. 2023. "Solar Energy Dependent Supercapacitor System with ANFIS Controller for Auxiliary Load of Electric Vehicles." *Energies* 16:2690. https://doi.org/10.3390/en16062690.

Razaq, A., L. Nyholm, M. Sjodin, M. Stromme, and A. Mihranyan. 2012. "Paper-based Energy-storage Devices Comprising Carbon Fiber-reinforced Polypyrrole-cladophora Nanocellulose Composite Electrodes." *Advanced Energy Materials* 2 (4): 445–454. https://doi.org/10.1002/aenm.201100713.

Shaheer, Khan, and Ataur Rahman. 2021. "The Impact of ZnO/PVA Solar Film on the Ehnacement of Organic Solar Panel Efficiency." *Journal of Material Research Express* 8:1–12.

Sun, H. M., L. Y. Cao, and L. H. Lu. 2012. "Bacteria Promoted Hierarchical Carbon Materials for High-performance Supercapacitor." *Energy & Environmental Science* 5 (3): 6206–6213. https://doi.org/10.1039/c2ee03407g.

Wu, Q., Y. Xu, Z. Yao, A. Liu, and G. Shi. 2010. "Supercapacitors Based on Flexible Graphene/Polyaniline Nanofiber Composite Films." *ACS Nano* 4 (4): 1963–1970. https://doi.org/10.1021/nn1000035.

Xia, J., F. Chen, J. Li, and N. Tao. 2009. "Measurement of the Quantum Capacitance of Graphene." *Nature Nanotechnology* 4 (8): 505. https://doi.org/10.1038/nnano.2009.177.

Yu, G. H., L. B. Hu, M. Vosgueritchian, H. L. Wang, X. Xie, J. R. McDonough, X. Cui, Y. Cui, and Z. N. Bao. 2011. "Solution-Processed Graphene/MnO_2 Nanostructured Textiles for High-performance Electrochemical Capacitors." *Nano Letters* 11 (7): 2905–2911. https://doi.org/10.1021/nl2013828.

Zhang, L. L., S. Li, J. T. Zhang, P. Z. Guo, J. T. Zheng, and X. S. Zhao. 2010. "Enhancement of Electrochemical Performance of Macroporous Carbon by Surface by Surface Coating of Polyaniline." *Chemistry of Materials* 22 (3): 1195–1202. https://doi.org/10.1021/cm902685m.

Zhang, L. L., and X. S. Zhao. 2009. "Carbon-based Materials as Supercapacitor Electrodes." *Chemical Society Reviews* 38 (9): 2520–2531. https://doi.org/10.1039/b813846j.